

Nonequilibrium fractional Hall response after a topological quench

F. Nur Ünal,^{1,2,*} Erich J. Mueller,¹ and M. Ö. Oktel²

¹Laboratory of Atomic and Solid State Physics, Cornell University, Ithaca, New York 14853, USA

²Department of Physics, Bilkent University, 06800, Ankara, Turkey

(Received 12 August 2016; published 7 November 2016)

We theoretically study the Hall response of a lattice system following a quench where the topology of a filled band is suddenly changed. In the limit where the physics is dominated by a single Dirac cone, we find that the change in the Hall conductivity is two-thirds of the quantum of conductivity. We explore this universal behavior in the Haldane model and discuss cold-atom experiments for its observation. Beyond the linear response, the Hall effect crosses over from fractional to integer values. We investigate finite-size effects and the role of harmonic confinement.

DOI: [10.1103/PhysRevA.94.053604](https://doi.org/10.1103/PhysRevA.94.053604)

I. INTRODUCTION

What happens when a system is suddenly driven between two topologically different phases? Several authors have tried to answer this question in the context of Chern insulators [1–7]. Aspects of the original topology survive the quench, but most physical observables (edge currents, Hall conductivity) appear to be nonuniversal. Here, we study the nonequilibrium Hall response following a quench where the mass term of a single Dirac cone changes sign and apply these results to understanding quenches in Chern insulators. Such nonequilibrium questions are at the forefront of research into topological systems [1–9]. We find that, for symmetric quenches dominated by a single Dirac cone, the Hall conductivity universally changes by $2e^2/3h$, which is two-thirds of the quantum of conductivity.

We argue that this nonequilibrium topological response can be observed in cold-atom experiments. Jotzu *et al.* [10] recently implemented the Haldane model [11] by using fermionic potassium atoms and observed transitions between ordinary insulators (OIs) and Chern insulators (CIs). They are capable of quenching between these phases. Here, we analyze these transitions and discuss a protocol for observing the nonequilibrium fractional Hall response.

To establish our central result, we first analytically calculate the nonequilibrium response for a single Dirac cone in a two-band model. We then show that the universal fractional Hall response of a single Dirac cone appears in quenches of the Haldane model. We consider both an infinite geometry as well as a strip configuration. The latter configuration lets us study the evolution of the edges modes. In addition to linear response, we explore the full time dynamics of this system in an electric field. We find that the currents perpendicular to the field are time dependent. At short times, they are consistent with the fractional Hall conductivity predicted by our linear-response theory. At long times, they instead correspond to an integer Hall response.

One important question for observing these effects is the role of finite system size. We find that, for narrow strips, the equilibrium Hall response deviates from the integral value predicted by bulk calculations. The deviation vanishes as the inverse of the system size. A related question is the role of harmonic confinement. Remarkably, we find that even though

the edges of a harmonically trapped cloud are metallic, one can observe a quantized Hall response. Furthermore, we show that, by analyzing currents inside the trapped cloud, one can infer the Hall conductance, without applying an electric field. When discussing the neutral atomic systems we will continue to use the language of electrodynamics: The electric field is a force, current is particle current, and the charge is simply unity.

The paper is organized as follows: In the next section, we calculate the Hall response of a single Dirac cone following a quench that inverts its mass sign. Section III generalizes this discussion to the Haldane model. In Sec. III B, we analyze the nonlinear characteristics of the out-of-equilibrium Hall response. Then in Sec. III C, we consider a strip configuration and investigate finite-size effects. Section IV focuses on the effect of a harmonic confinement on the Hall conductivity of a strip and discusses correspondences to cold-atom experiments. We conclude our discussion with Sec. V.

II. SINGLE DIRAC CONE

Near a topological transition of a 2D system, the low-energy physics is described by a massive Dirac model [11–13]. We parametrize the static Hamiltonian by two quantities: the gap Δ and the “speed of light” c ,

$$\mathcal{H}(\vec{k}) = \begin{pmatrix} \Delta & cke^{i\theta} \\ cke^{-i\theta} & -\Delta \end{pmatrix}, \quad (1)$$

where $ke^{i\theta} = k_x + ik_y$ expresses the 2D momentum as a complex number. When $\Delta = 0$, the spectrum consists of a gapless Dirac cone at $\vec{k} = 0$. For nonzero Δ , a gap with magnitude $2|\Delta|$ opens at zero momentum. The energies $\varepsilon_n = (-1)^n(\Delta^2 + c^2k^2)^{1/2}$ for the band index $n = 1, 2$ are independent of the sign of the gap (mass). The corresponding eigenstates are

$$u_n(\vec{k}) = \frac{1}{N_n(\vec{k})} \begin{pmatrix} (-1)^n e^{i\theta} ck/\Delta \\ \sqrt{1 + (ck/\Delta)^2} - (-1)^n \end{pmatrix}, \quad (2)$$

where

$$N_n(\vec{k}) = \sqrt{2} \sqrt{1 + \left(\frac{ck}{\Delta}\right)^2 - (-1)^n \sqrt{1 + \left(\frac{ck}{\Delta}\right)^2}}$$

*fatmanur@bilkent.edu.tr

is the normalization. One imagines that the negative-energy modes are filled, and the positive-energy modes are empty. The contribution to the Hall conductivity from these low-energy modes can be calculated from the Chern number C via $\sigma_H = Ce^2/h$ [14]. The Chern number is given by

$$C_n = \frac{1}{2\pi} \int d^2k \Omega_n(\vec{k}), \quad (3)$$

where the Berry curvature is

$$\Omega_n(\vec{k}) = -i \langle \partial_{\vec{k}} u_n(\vec{k}) | \times | \partial_{\vec{k}} u_n(\vec{k}) \rangle = \frac{(-1)^{n+1} c^2 \Delta}{2(\Delta^2 + c^2 k^2)^{3/2}}. \quad (4)$$

The Berry curvature is odd in the gap parameter, and the Chern numbers of the cones $C = \pm 1/2$ depend on the sign of Δ , even though the energy spectrum does not. The Chern number for a given band must be an integer, so the modes neglected in the low-energy description must also supply a half-integer Chern number. We are envisioning a quench which does not affect these higher-energy modes, and their contribution to the Hall conductivity will not change during the quench.

We imagine suddenly flipping the sign of the Δ . The probability $P_n(\vec{k})$ of a particle of momentum k being found in the n th band following this quench is simply the inner product between $u_1(\vec{k})$ and $\bar{u}_n(\vec{k})$, where \bar{u}_n is given by Eq. (2) with $\Delta \rightarrow -\Delta$. This yields

$$P_1(\vec{k}) = \frac{c^2 k^2}{\Delta^2 + c^2 k^2}, \quad P_2(\vec{k}) = \frac{\Delta^2}{\Delta^2 + c^2 k^2}. \quad (5)$$

After the quench, the system is in a nonequilibrium state. Hence, each k point contributes to the Hall conductivity with its Berry curvature weighted by its occupation probability [3,7],

$$\sigma_{H,\text{neq}} = \frac{e^2}{h} C_{\text{neq}} = \frac{e^2}{2\pi h} \sum_n \int d^2k P_n(\vec{k}) \Omega_n(\vec{k}). \quad (6)$$

Any effects from coherences between the bands average out over a time $\tau \sim h/\Delta$, and can be neglected in linear response. Equation (6) reduces to the usual Thouless, Kohmoto, Nightingale, and den Nijs (TKNN) formula [14] for the ground state where the occupation probability of the lowest band is one at each k and the higher bands are completely empty. For partially filled bands, the dimensionless Hall conductivity C_{neq} is clearly not quantized and can take any value. However, in a mass-sign-inverting quench, the symmetry between initial and final states will yield a universal result. In particular for our case, the integrals in Eq. (6) are elementary and

$$C_{\text{neq}} = \frac{1}{3} - \frac{1}{6} = \frac{1}{6}. \quad (7)$$

Here, the first (second) term is the contribution coming from the lower (upper) band. This fractional Hall response is independent of Δ . Although the Berry curvatures and the number of excited particles are highly sensitive to the value of the gap, they remarkably balance each other in symmetric quenches and one always ends up with 1/6-Hall response. If the quench is performed in the opposite direction, C_{neq} changes sign to $-1/6$. Since the initial Chern number was $\pm 1/2$, the change in the Hall conductivity in such symmetric quenches is always $\pm 2/3$.

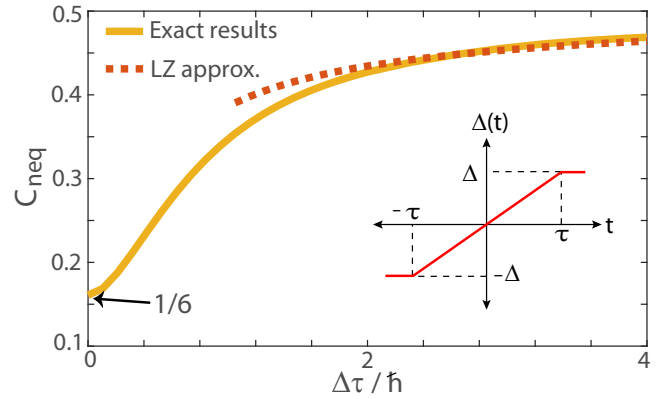


FIG. 1. Nonequilibrium Hall conductivity, C_{neq} , of a single Dirac cone following a ramp of the gap from $-\Delta$ to Δ in time 2τ as shown in inset. C_{neq} is measured in units of e^2/h , and the product $\Delta\tau/\hbar$ is dimensionless. In the sudden-quench limit ($\tau = 0$), $C_{\text{neq}} = 1/6$ and as $\Delta\tau \rightarrow \infty$, $C_{\text{neq}} \rightarrow 1/2$. The dashed line shows prediction of the LZ theory from Eq. (9).

For completeness, we also consider sweeps with finite rate where the gap is linearly ramped from $-\Delta$ to Δ within time 2τ as illustrated in the inset of Fig. 1. We solve the Schrödinger equation

$$i\hbar \frac{\partial}{\partial t} |\Psi(\vec{k}, t)\rangle = \mathcal{H}(\vec{k}, t) |\Psi(\vec{k}, t)\rangle, \quad (8)$$

assuming the lower band is initially full. The adiabatic eigenstates of the Hamiltonian traverse an avoided crossing as the sign of the gap changes. At each k , there is an independent Landau-Zener (LZ) problem, with adiabaticity parameter $\eta_k = c^2 k^2 \tau / \hbar \Delta$. When $\eta_k \gg 1$, the particle remains in the lower band, while $\eta_k \ll 1$ it transitions with the probabilities in Eq. (5). Adiabaticity always holds for modes with sufficiently large k . If the gap is large, $\Delta \gg \hbar/\tau$, then the majority of the modes which contribute to the Hall conductance will be in that region. One can then use the LZ approximation, $P_2(\vec{k}, \tau) = e^{-\pi c^2 k^2 \tau / \hbar \Delta}$ which yields a Hall conductivity

$$C_{\text{neq}}^{\text{LZ}} = -\frac{1}{2} + \pi \sqrt{\frac{\Delta\tau}{\hbar}} e^{\pi \Delta\tau/\hbar} \text{erfc}\left(\sqrt{\pi \frac{\Delta\tau}{\hbar}}\right). \quad (9)$$

Here, erfc is the complementary error function. For a general value of $\Delta\tau/\hbar$, we numerically calculate the excitation probabilities and the Hall conductivity (see Fig. 1). We see that, for slow sweeps, the Hall conductivity saturates at $C_{\text{neq}} = 1/2$, while rapid quenches yield $C_{\text{neq}} = 1/6$. For $\Delta\tau/\hbar > 2$, the Hall conductivity is well approximated by the LZ result (9).

Our result, that the contribution to the nonequilibrium Hall conductivity from a single Dirac cone is 1/6 of the quantum of conductivity, implies that one will see this same fraction in small quenches of any topological lattice system. To illustrate this universality, we study the Haldane model.

III. THE HALDANE MODEL

A. Infinite system

The Haldane model is a simple yet realistic topological lattice model which realizes a quantum Hall effect in the

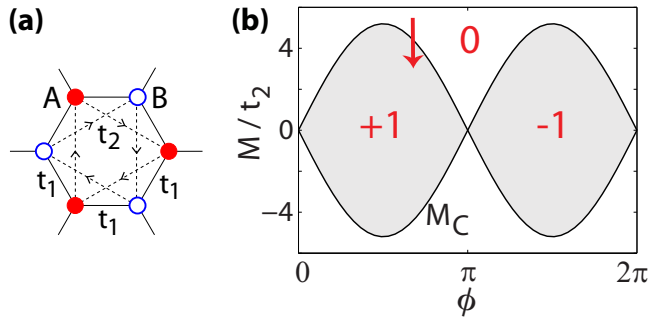


FIG. 2. Haldane model. (a) Illustration of the matrix elements of the tight-binding Hamiltonian in Eq. (10); hoppings t_1 , $t_2 e^{\pm i\phi}$ and bias $2M$ between A (dark) and B (light) sublattices. (b) Phase diagram showing the Chern number of the lowest band $C = 0, \pm 1$. The arrow indicates the quench studied in the text. Bands touch at a single Dirac point for $M_C = \pm t_2 3\sqrt{3} \sin \phi$.

absence of a net magnetic field [11]. Recent cold-atom realizations [4,10,15,16] provide an ideal platform to study out-of-equilibrium topological phenomena. The static Haldane Hamiltonian describes noninteracting fermions on a honeycomb lattice [see Fig. 2(a)],

$$\begin{aligned} \mathcal{H} = & -t_1 \sum_{\langle ij \rangle} a_i^\dagger a_j - t_2 \sum_{\langle\langle ij \rangle\rangle} e^{\pm i\phi} a_i^\dagger a_j \\ & + M \sum_A a_i^\dagger a_i - M \sum_B a_i^\dagger a_i, \end{aligned} \quad (10)$$

where a_i^\dagger (a_i) creates (annihilates) a fermion at site i . The first term is the nearest-neighbor hopping between the two sublattices, and the second is the next-nearest-neighbor intrasublattice hopping which breaks time-reversal symmetry (TRS). The arrows in Fig. 2(a) represent hopping directions for which the phase gain is positive. An energy offset M of A and B sublattices breaks inversion symmetry (IS). The corresponding phase diagram is given in Fig. 2(b) where we take $|t_2/t_1| \leq 1/3$ to allow the bands to touch but not to overlap [11]. When both ϕ and M are zero, the spectrum is graphene like with two Dirac cones in the Brillouin zone. Breaking TRS opens a gap at the two Dirac points, yielding topological bands with Chern numbers $C = \pm 1$. Opening a gap by breaking IS, on the other hand, results in an OI where the Chern numbers vanish. By tuning the competition between the two symmetry-breaking terms, one can engineer a topological transition involving only one of the Dirac cones. The critical energy offset of the transition is given by $M_C = \pm t_2 3\sqrt{3} \sin \phi$. The analysis in Sec. II suggests that a symmetric quench across this boundary will yield a universal nonequilibrium Hall response.

We now calculate the Hall response of the Haldane model following a quench that changes the mass sign of one of the Dirac cones in the Brillouin zone. As is simplest in experiments, we quench the energy offset M , but a quench of ϕ or t_2 would also work. We start with a completely filled lower band at energy offset $M_i = M_C + \Delta M$ for $\phi = 0.6\pi$ and $t_2 = 0.1t_1$, where the system is in OI state for $\Delta M > 0$. These lattice parameters are representative: we find equivalent results for other parameters. The first Dirac cone initially contributes a Chern number of $-1/2$ where the second one

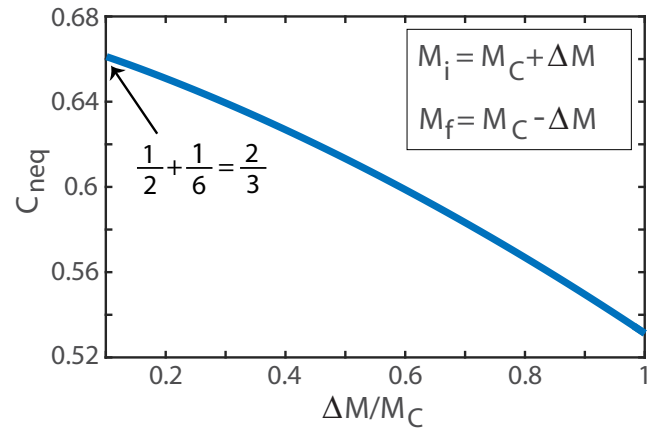


FIG. 3. Nonequilibrium Hall response of the Haldane model. The energy offset M is suddenly quenched from $M_i = M_C + \Delta M$ to $M_f = M_C - \Delta M$, where $M_C = t_2 3\sqrt{3} \sin \phi$ is the topological transition point. Here $\phi = 0.6\pi$ and $t_2 = 0.1t_1$. For small quenches one reaches the fractional regime in which $C_{\text{neq}} \rightarrow 2/3$.

contributes $1/2$, hence the Chern number is zero. We then suddenly change the sublattice bias to $M_f = M_C - \Delta M$, as illustrated in Fig. 2(b) with the red arrow, and calculate the excitation probabilities at each k in the Brillouin zone. By multiplying the Berry curvatures of the final bands with the occupation probabilities, we calculate the Hall conductivity as in Fig. 3.

In the limit of $\Delta M \ll M_C$, the transition involves only the first Dirac cone. Since particles near the second Dirac cone are not excited, they continue to contribute $1/2$ to the Chern number. On the other hand, the mass of the first Dirac cone changes sign, so its contribution to the Hall response is $1/6$ as in Sec. II. Together they add up to a Hall response of $2/3$, as seen in Fig. 3. Note that, in this limit, the actual number of particles excited to the upper band is small, but the change in the Hall conductivity is still $2/3$ because the Berry curvature is peaked at the Dirac cone. There are no contributions from the rest of the Brillouin zone because the Berry curvature is negligible and no particles are excited. For larger quenches ($\Delta M \sim M_C$), the Hall conductivity deviates from $2/3$ due to the excitations at the second Dirac cone. For quenches in the other direction, from CI phase to OI phase, the Hall conductivity becomes $C_{\text{neq}} = 1/2 - 1/6 = 1/3$ where the contribution of the first Dirac cone comes with a minus sign.

Experimentally, the local Berry curvature of the bands can be probed by using wave packets [17], which is the measurement of choice in the Zurich experiment [10]. In this method, the wave packet is moved through the Brillouin zone sampling the transverse drift in regions with significant curvature. In quenches on the Haldane model, the action takes place mostly around one of the Dirac cones. If the systems is quenched while the wave packet is passing through the Dirac cone of interest, the resulting transverse drift will reveal the contribution of that Dirac cone alone, namely $1/6$. Since the observation of the universal $1/6$ Hall response does not require a Haldane model, but just the presence of a Dirac cone, it should be also accessible in the hexagonal lattices of

the Hamburg [4] and Munich groups [15] as long as one can isolate the contribution of a single Dirac cone. In practice, extracting the Chern number from such experiments requires attention to several technical details [5,10,17–19]. We discuss an alternative approach in Sec. IV.

B. Beyond linear response

In an equilibrium state, where the bands are either completely filled or empty, the occupation probability at each point in the Brillouin zone does not change when a force is applied [14]. However, in a nonequilibrium state, the nonuniform distribution will evolve as forces are applied, leading to pronounced nonlinearities in the Hall response. Here we characterize these nonlinearities. Linear response should be valid when the impulse imparted on the atoms $I = E\Delta t$ is small compared with the width of the Dirac cone Δ/c . Here we relax this constraint but still take $E \ll \Delta^2$. In this regime band coherences can be neglected, and one does not encounter the Zitterbewegung related effects found in Ref. [5] when they considered delta-function impulses.

An infinitesimal impulse $dI\hat{y}$ shifts a particle in the n th band with a momentum \vec{k} to $\vec{k} + dI\hat{y}$ and shifts its center of mass in the transverse direction by $dX = \Omega_n(\vec{k})dI$. The total displacement of the cloud is found by adding up the contribution from each (n, \vec{k}) mode; weighted by the probability of occupation $P_n(\vec{k})$. The response to a finite impulse is then calculated by adding up these infinitesimals,

$$X(I) = \frac{1}{2\pi} \int_0^I dI' \sum_n \int_{BZ} d^2k P_n(\vec{k} - I'\hat{y}) \Omega_n(\vec{k}). \quad (11)$$

The rate of change of this transverse displacement gives the Hall conductivity $\sigma_H = \partial X/\partial I$.

As in Sec. III A, we quench the system from the ground state of the OI phase at $M_i = M_C + \Delta M$ to the CI phase at $M_f = M_C - \Delta M$ (where $C = 1$) with $t_2 = 0.1t_1$ and $\phi = 0.6\pi$. We numerically calculate the final Berry curvatures $\Omega_n(\vec{k})$ and the probability distributions within the bands $P_n(\vec{k})$. We then apply an impulse $I\hat{y}$ which shifts the probability distributions according to Eq. (11). As seen in Fig. 4, the resulting Hall conductivity $\sigma_H = \partial X/\partial I$ depends on the applied impulse.

We observe a crossover from a fractional Hall response to an integer response. For large impulses, the excited particles move away from the Dirac point towards k values with negligible curvature. The lower band becomes again completely filled around the Dirac cone and the upper band completely empty. Hence, the Hall response approaches that of the equilibrium system ($C = 1$ in this case). In Fig. 4, we consider two different values of ΔM . For smaller ΔM , particle excitations and curvature are more confined around the Dirac point, resulting in a smaller linear-response regime.

In experiments on equilibrium states, larger impulses are almost always favorable: The bigger the impulse, the larger the transverse drift and hence the larger the signal. In a nonequilibrium setting, however, there is a tension between the desire to have a large signal, and the desire to be in the linear-response regime. The strength of the impulse should be chosen carefully.

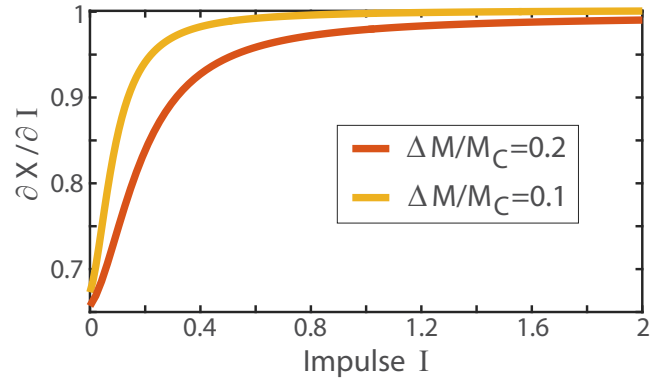


FIG. 4. Nonlinear Hall response $C_{\text{neq}} = \partial X/\partial I$ following a quench for transverse displacement X resulting from an impulse I . The parameters are adimensionalized by using the unit length of the lattice. The system is quenched between states ΔM around the transition point M_C as detailed in the text. The Hall response of a nonequilibrium system saturates to equilibrium result ($C = 1$ in this case) for large impulse. The linear-response regime shrinks for decreasing ΔM .

Up to this point we have been considering an experiment in which the fermionic cloud is initially in its ground state, and hence the Brillouin zone is uniformly filled. One could imagine other scenarios in which this fractional quantized conductance could be explored. For example, one could fill only the states near the Dirac cone (those with $k \lesssim \Delta/c$). In that case, one could observe the 1/6 Hall response of that Dirac cone. Of course, if the spread of the cloud in k space is too small, or too large, a nonuniversal value would be found. Many of the Haldane model experiments in Zurich have utilized such partially filled bands [10].

C. Strip geometry

The energy spectrum of a finite topological system is fundamentally different than the infinite system due to the presence of protected edge modes. In this section, we investigate how edge states modify both the equilibrium and nonequilibrium Hall response. We find that, for sufficiently wide strips, our results from bulk calculations hold. We also set up notation for exploring the spatial distribution of currents in a harmonic trap. In Sec. IV, we show that these currents can be used as a probe of the Hall effect.

We take the system to be infinite in the x direction and finite in the y direction with an armchair termination. We define a “layer” index for each site, which corresponds to its y position as shown in Fig. 5. Under a uniform electric field $E\hat{y}$ in the finite direction, a Hall current J_H flows along the strip in the x direction.

Our Hamiltonian can be expressed as $\mathcal{H} = -\sum_{ij} t_{i \rightarrow j} a_i^\dagger a_j + M \sum_A a_i^\dagger a_i - M \sum_B a_i^\dagger a_j$. The matrix element $t_{i \rightarrow j}$ is equal to t_1 for neighboring sites, $t_2 e^{\pm i\phi}$ for next-neighbor sites, and 0 for all others. The current from site i to j is then

$$\mathcal{J}_{i \rightarrow j} = 2\text{Im}\{t_{j \rightarrow i} \langle a_i^\dagger a_j \rangle\}. \quad (12)$$

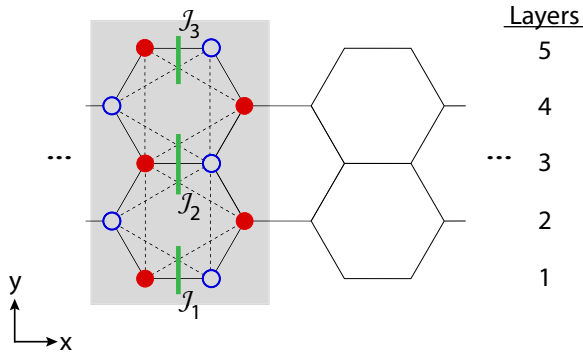


FIG. 5. Haldane strip with armchair termination, for parameters introduced in Fig. 2(a). The unit cell is given by the shaded area. We label the layers in the finite y direction. Green (thick vertical) lines represent how nearest- and next-nearest-neighbor hoppings are assigned into these layers to calculate the current density \mathcal{J}_ℓ .

To quantify the spatial distribution of currents, we group the currents according to the layers of i and j . For each odd integer ℓ , we define \mathcal{J}_ℓ to be the sum of currents either originating from or ending at the ℓ^{th} layer, at some fixed x position in the unit cell (see Fig. 5). In an OI state, $J_H = \sum \mathcal{J}_\ell$ is always zero even though there may be nonzero currents in individual layers. For a CI phase, however, J_H is finite in the presence of a nonzero electric field. The Hall conductivity of the strip is then $\sigma_H^s = \frac{1}{W} \frac{\partial J_H}{\partial E}$, where W is the width of the strip.

Cold-atom experiments can explore strips of varying width, even as small as two layers [20]. Thus, they are well suited to quantifying finite-size effects. To analyze these effects in accessing bulk topological properties, here we first consider equilibrium Hall response of a strip in the CI regime.

We take an L -layer strip with $M = 0$, $t_2 = 0.1t_1$, and $\phi = 0.6\pi$. Here, the edge states are well separated from the bulk, and we take the Fermi energy to lie in the bulk gap. An infinite system with these parameters would have a Chern number of 1. We apply an electric field and measure the resulting J_H . Due to the presence of the hallmark edge states, we find that σ_H^s is somewhat smaller than one would expect from the bulk calculations (see Fig. 6). The deviation falls off as $1/L$ for large L . This is sensible, because the ratio of edge to bulk modes falls off with this same power. We repeat this calculation at $M = M_C - 0.1$, where the bulk gap is smaller. Given the larger extent of the edge modes, it is not surprising that we find a larger deviation from bulk behavior.

We now consider a wide strip and study our symmetric quenches of Sec. III A. We start with a ground state as before in the OI phase at $M_i = M_C + \Delta M$ with the same parameters in the previous section: $t_2 = 0.1t_1$ and $\phi = 0.6\pi$. We numerically calculate the initial eigenstates for $L = 201$ layers. We then quench the system into the CI phase at $M_f = M_C - \Delta M$ and find the occupation probabilities of the final eigenstates by calculating overlaps with the final eigenstates.

To explore the Hall response, we then add a small electric field $E\hat{y}$ and calculate the currents in our nonequilibrium state. We find that, for small quenches $\Delta M/M_C = 0.1$ and 0.2 , the resulting Hall response of the strip is $\sigma_H^s = 0.66$ and 0.65 respectively. Hence, in small quenches symmetric around the

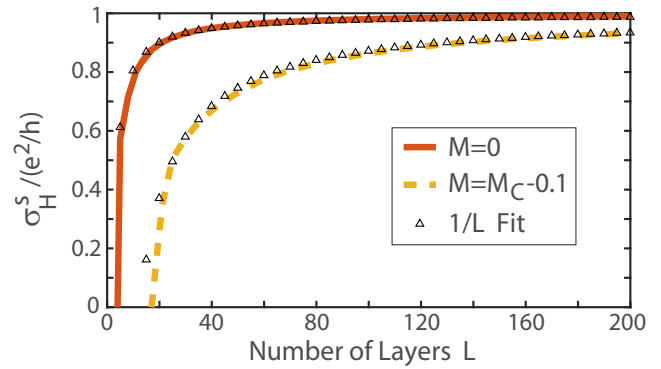


FIG. 6. Equilibrium Hall conductivity of the strip as a function of number of layers in the finite direction. The system is in CI state at $M = 0$ and $M = M_C - 0.1$, for $t_2 = 0.1t_1$ and $\phi = 0.6\pi$. Hall conductivity approaches to the quantized bulk value as $1/L$ for increasing strip width.

transition point, the Hall conductivity of a strip successfully reproduces the infinite-system result of $2/3$.

IV. HARMONIC TRAP

Nearly all cold-atom experiments include a harmonic trap. Naively, this potential complicates the search for topological physics: Even if the center of the cloud is a CI, the edge is always metallic. The metallic edges wash out any potential signals from edge modes, and one might expect them to dominate the Hall response, yielding nonuniversal, nonquantized results. In this section, we investigate a Haldane model with harmonic confinement added. We find equilibrium currents whose spatial distribution reveals the underlying topological physics. We discuss protocols for detecting these currents and using them to infer the quantized Hall response.

We take the formalism of Sec. III C and add a potential $H = \sum_i \frac{1}{2} m \omega^2 y_i^2$ where y_i is the y position of the i th site. We consider this unidirectional harmonic potential because it simplifies analyzing the currents. In a cylindrically symmetric harmonic trap, one would observe similar results, with the radial direction playing the role of y . In Fig. 7(a), we show the local density of states of this system, taking $M = 0$, $t_2 = 0.2t_1$, $\phi = 0.5\pi$, and $\hbar\omega = 0.09t_1$. We take the chemical potential to lie in the bulk gap at the center of the cloud, which will locally be in the CI phase. The metallic edges are characterized by the finite density of states at the Fermi level.

In Fig. 7(b), we show the local equilibrium current \mathcal{J}_ℓ as a function of position in finite direction in the absence of an electric field. In the insulating region, one sees a current which grows linearly with position in a trap. On the metallic edges, there are large counterpropagating currents. The net current vanishes. The bulk currents are nothing but the quantized anomalous Hall currents coming from the topological band and the trapping potential. The trap is equivalent to a spatially dependent electric field $E_y = -m\omega^2 y/e$. Within a local density approximation this leads to a local current density $j_x = \sigma_H E_y = -eCm\omega^2 y/h$. Indeed, the slope of the line in Fig. 7(b) matches this prediction.

We propose a simple protocol to measure these local currents. One begins with a noninteracting spin polarized Fermi

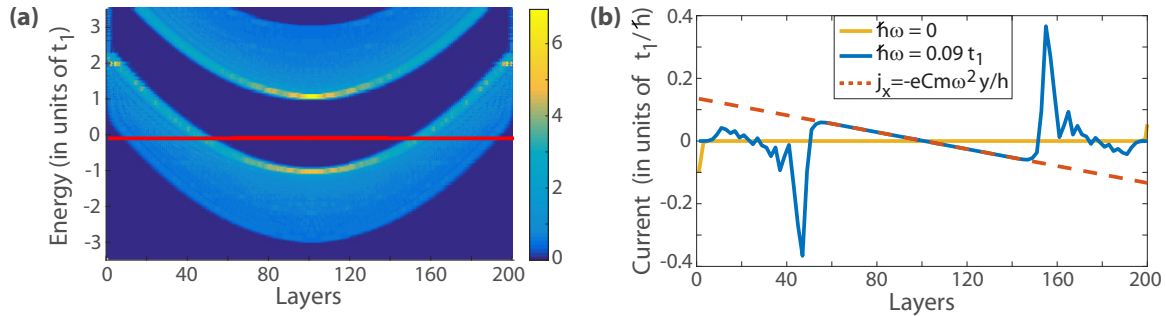


FIG. 7. Effect of a harmonic trap with $\hbar\omega = 0.09t_1$ in the finite direction for $M = 0$, $t_2 = 0.2t_1$, and $\phi = 0.5\pi$. (a) Local density of states along the finite direction where the center is a CI and the edges are metallic. The Fermi energy is indicated with the red line. (b) Current density flowing along the strip with (dark line) and without (light line) trap, in the absence of an electric field. The force exerted by the trap $F_y = -m\omega^2 y$ results in anomalous currents in the central topological region according to $j_x = eCF_y/h$ (dashed line).

gas in a situation like Fig. 7(a). Using standard techniques [21–24], one locally flips the spins of a small number of atoms. Local currents will be apparent in the motions of these spins. Cold-atom experiments can explore not only the average current, but also the spatial distribution of the currents [20,25]. This extra information can disentangle the contributions from the metallic edges and the bulk. Furthermore, if the system is to be quenched, one can still access the Hall response of the topological central region even in the presence of a harmonic trap.

V. SUMMARY

Out-of-equilibrium systems exhibit new topological phenomena which have no equilibrium counterpart. Here, we report a universal fractional value of the Hall conductivity when the mass sign of a single Dirac cone in a two-band model is suddenly changed. The energy spectrum is independent of the sign of the gap while the eigenstates are sensitive to it. We find that this symmetry results in a contribution to the Hall response of $|C_{\text{neq}}| = 1/6$ independently from the actual value

of the gap. By studying the Haldane model, we illustrate the universality of this result: Any symmetric topological quench dominated by a single Dirac cone will observe this fractional Hall response. We find that the out-of-equilibrium response is highly nonlinear in the impulse. To connect with experiments [10], we explore finite-size effects, and the role of harmonic confinement. By studying finite strips of size L , we determine that there are corrections to the quantized conductance which scale as $1/L$. Including the harmonic confinement, we find the equilibrium bulk currents which reveal the quantized Hall effect. We propose an experiment for detecting these currents.

ACKNOWLEDGMENTS

F.N.Ü. is supported by The Scientific and Technological Research Council of Turkey (TÜBİTAK). M.Ö.O. would like to thank the American Physical Society for support via the International Research Travel Award Program, and LASSP at Cornell University for their hospitality. E.J.M. acknowledges support from NSFPHY-1508300 and ARO-MURI Non-Equilibrium Many-Body Dynamics W911NF-14-1-0003.

-
- [1] Luca D’Alessio and Marcos Rigol, Dynamical preparation of Floquet Chern insulators, *Nat. Commun.* **6**, 8336 (2014).
- [2] M. D. Caio, N. R. Cooper, and M. J. Bhaseen, Quantum Quenches in Chern Insulators, *Phys. Rev. Lett.* **115**, 236403 (2015).
- [3] P. Wang, M. Schmitt, and S. Kehrein, Universal nonanalytic behavior of the Hall conductance in a Chern insulator at the topologically driven nonequilibrium phase transition, *Phys. Rev. B* **93**, 085134 (2016).
- [4] N. Fläschner, D. Vogel, M. Tarnowski, B. S. Rem, D.-S. Lühmann, M. Heyl, J. C. Budich, L. Mathey, K. Sengstock, and C. Weitenberg, Observation of a dynamical topological phase transition, [arXiv:1608.05616](https://arxiv.org/abs/1608.05616).
- [5] J. H. Wilson, J. C. W. Song, and G. Refael, Persistent Hall response in a quantum quench, [arXiv:1603.01621](https://arxiv.org/abs/1603.01621).
- [6] Y. Hu, P. Zoller, and J. C. Budich, Dynamical Buildup of a Quantized Hall Response from Non-Topological States, *Phys. Rev. Lett.* **117**, 126803 (2016).
- [7] M. D. Caio, N. R. Cooper, and M. J. Bhaseen, Hall response and edge current dynamics in Chern insulators out of equilibrium, *Phys. Rev. B* **94**, 155104 (2016).
- [8] M. S. Foster, V. Gurarie, M. Dzero, and E. A. Yuzbashyan, Quench-Induced Floquet Topological p -Wave Superfluids, *Phys. Rev. Lett.* **113**, 076403 (2014).
- [9] H. Dehghani, T. Oka, and A. Mitra, Out-of-equilibrium electrons and the Hall conductance of a Floquet topological insulator, *Phys. Rev. B* **91**, 155422 (2015).
- [10] G. Jotzu, M. Messer, R. Desbuquois, M. Lebrat, T. Uehlinger, D. Greif, and T. Esslinger, Experimental realization of the topological Haldane model with ultracold fermions, *Nature (London)* **515**, 237 (2014).
- [11] F. D. M. Haldane, Model for a Quantum Hall Effect without Landau Levels: Condensed-Matter Realization of the “Parity Anomaly,” *Phys. Rev. Lett.* **61**, 2015 (1988).
- [12] D. Xiao, M.-C. Chang, and Q. Niu, Berry phase effects on electronic properties, *Rev. Mod. Phys.* **82**, 1959 (2010).
- [13] M. Z. Hasan and C. L. Kane, Colloquium: Topological insulators, *Rev. Mod. Phys.* **82**, 3045 (2010).

- [14] D. J. Thouless, M. Kohmoto, M. P. Nightingale, and M. den Nijs, Quantized Hall Conductance in a Two-Dimensional Periodic Potential, *Phys. Rev. Lett.* **49**, 405 (1982).
- [15] L. Duca, T. Li, M. Reitter, I. Bloch, M. Schleier-Smith, and U. Schneider, An Aharonov-Bohm interferometer for determining Bloch band topology, *Science* **347**, 288 (2015).
- [16] N. Goldman, J. C. Budich, and P. Zoller, Topological quantum matter with ultracold gases in optical lattices, *Nat. Phys.* **12**, 639 (2016).
- [17] H. M. Price and N. R. Cooper, Mapping the Berry curvature from semiclassical dynamics in optical lattices, *Phys. Rev. A* **85**, 033620 (2012).
- [18] M. Aidelsburger, M. Lohse, C. Schweizer, M. Atala, J. T. Barreiro, S. Nascimbène, N. R. Cooper, I. Bloch, and N. Goldman, Measuring the Chern number of Hofstadter bands with ultracold bosonic atoms, *Nat. Phys.* **11**, 162 (2015).
- [19] N. Goldman, G. Jotzu, M. Messer, F. Görg, R. Desbuquois, and T. Esslinger, Creating topological interfaces and detecting chiral edge modes in a two-dimensional optical lattice, *Phys. Rev. A* **94**, 043611 (2016).
- [20] M. Atala, M. Aidelsburger, M. Lohse, J. T. Barreiro, B. Paredes, and I. Bloch, Observation of chiral currents with ultracold atoms in bosonic ladders, *Nat. Phys.* **10**, 588 (2014).
- [21] T. Fukuhara, A. Kantian, M. Endres, M. Cheneau, P. Schauß, S. Hild, D. Bellem, U. Schollwöck, T. Giamarchi, C. Gross, I. Bloch, and S. Kuhr, Quantum dynamics of a mobile spin impurity, *Nat. Phys.* **9**, 235 (2013).
- [22] M. R. Matthews, B. P. Anderson, P. C. Haljan, D. S. Hall, C. E. Wieman, and E. A. Cornell, Vortices in a Bose-Einstein Condensate, *Phys. Rev. Lett.* **83**, 2498 (1999).
- [23] A. P. Chikkatur, A. Görlitz, D. M. Stamper-Kurn, S. Inouye, S. Gupta, and W. Ketterle, Suppression and Enhancement of Impurity Scattering in a Bose-Einstein Condensate, *Phys. Rev. Lett.* **85**, 483 (2000).
- [24] K. C. Wright, L. S. Leslie, and N. P. Bigelow, Raman coupling of Zeeman sublevels in an alkali-metal Bose-Einstein condensate, *Phys. Rev. A* **78**, 053412 (2008).
- [25] S. Keßler and F. Marquardt, Single-site-resolved measurement of the current statistics in optical lattices, *Phys. Rev. A* **89**, 061601 (2014).